Breast Cancer Res Treat (2015) 149:577–585
DOI 10.1007/s10549-015-3268-8

PRECLINICAL STUDY

Germ line knockout of *IGFBP-3* reveals influences of the gene on mammary gland neoplasia

Marie-José Blouin · Miguel Bazile · Elena Birman · Mahvash Zakikhani · Livia Florianova · Olga Aleynikova · David R. Powell · Michael Pollak

Received: 5 November 2014 / Accepted: 7 January 2015 / Published online: 23 January 2015

Abstract Insulin-like growth factor binding protein-3 (IGFBP-3) is an important carrier protein for insulin-like growth factors (IGFs) in the circulation. IGFBP-3 antagonizes the growth-promoting and anti-apoptotic activities of IGFs in experimental systems, but in certain contexts can increase IGF bioactivity, probably by increasing its half-life. The goal of this study was to investigate the role of *IGFBP-3* in breast carcinogenesis and breast cancer metastasis. In the first part of the study, we exposed *IGFBP-3* knockout and wild-type female mice to dimethylbenz[*a*]anthracene (DMBA) and followed them for appearance of primary tumors for up to 13 months. In the second part, mice of each genotype received an IV injection of 4T1 mammary carcinoma cells and then lung nodules were counted. Our results show that *IGFBP-3* knockout mice developed breast tumors significantly earlier than the wild-type (13.9 ± 1.1 versus 22.5 ± 3.3 weeks, respectively, $P = 0.0144$), suggesting tumor suppression activity of *IGFBP-3*. In tumors of *IGFBP-3* knockout mice, levels of phospho-AKT^{Ser473} were increased compared to wild-type mice. The lung metastasis assay showed significantly more and larger lung nodules in *IGFBP-3* knockout mice than in wild-type mice. While we observed increased levels of IGFBP-5 protein in the *IGFBP-3* knockout mice, our findings suggest that this was not sufficient to completely compensate for the absence of IGFBP-3. Even though knockout of *IGFBP-3* is associated with only a subtle phenotype under control conditions, our results reveal that loss of this gene has measurable effects on breast carcinogenesis and breast cancer metastasis.

Keywords IGFBP-3 · DMBA · Carcinogenesis · Metastasis

M.-J. Blouin (✉) · M. Bazile · E. Birman · M. Zakikhani · M. Pollak
Lady Davis Institute for Medical Research of the Jewish General Hospital, Room E-423, 3755 Cote-Ste-Catherine Road, Montreal, QC H3T 1E2, Canada
e-mail: marie-jose.blouin@mail.mcgill.ca

L. Florianova
Department of Pathology, McGill University Health Center, McGill University, Montreal, QC, Canada

O. Aleynikova
Department of Pathology, Jewish General Hospital, Montreal, QC, Canada

D. R. Powell
Lexicon Pharmaceuticals Inc., The Woodlands, TX, USA

M. Pollak
Department of Oncology, McGill University, Montreal, QC, Canada

Introduction

Insulin-like growth factor binding proteins (IGFBPs) bind both IGF-1 and IGF-2 with high affinity and specificity, and modulate bioactivity of these growth factors [1–4]. IGFBP-3 has been identified as the major carrier of IGFs in the circulation and also plays a role in autocrine and paracrine growth control and apoptosis. It has been shown that exogenous IGFBP-3 can slow the growth of breast cancer and other tumor cells in culture by sequestration of IGFs, thus reducing their binding to receptors [5–8], and blocking their anti-apoptotic activity [9]. IGFBP-3 can also induce apoptosis and growth inhibition via IGF-1 independent mechanisms in various cell systems [3, 10–13]. IGFBP-3 was also shown to exert tumor growth inhibition by suppressing angiogenesis [14]. In addition, up-regulation of

IGFBP-3 may contribute to the anti-proliferative action of some of the agents recommended for chemoprevention [15–20] or chemotherapy [3, 21, 22].

Transgenic and knockout mouse models have been developed to characterize the roles of IGFBPs [23–26]. In general, IGFBP-3 knockout mice do not exhibit a distinct phenotype under standard conditions [27], but one study using a *c-myc*-driven transgenic prostate cancer model has shown that in the absence of IGFBP-3, castration-induced apoptosis is attenuated and metastasis is accelerated [28].

In this study, we used an IGFBP-3 knock-out model to determine the role of IGFBP-3 in a chemically induced mammary gland carcinogenesis model and in a metastasis model.

Materials and methods

Animals

IGFBP-3 knockout (KO) mice were generated at Lexicon Pharmaceuticals Inc., The Woodlands, TX, as previously described [29]: Heterozygous male and female mice on a 129/SvEv-C57BL/6 background were bred to generate *IGFBP-3* knockout and wild-type (WT) mice (which were used for the DMBA-induced mammary tumor study). To obtain IGFBP-3 KO mice on a pure Balb/c background for use in the metastasis assay, heterozygous *IGFBP-3* female mice were first bred with a Balb/c male mouse for more than 10 generations of backcrossing, and then homozygous *IGFBP-3* knockout and wild-type animal were generated. Primers for genotyping are shown in Table 1 as described [29]. All mice were maintained in a climate-controlled environment with conditions of 14 h light:10 h darkness, a temperature of 22 ± 2 °C, and a relative humidity of 30–60 %. Animal care and treatments were conducted in accordance with established guidelines and protocols approved by the Institute and McGill University's Animal Ethics Committee.

DMBA treatment and follow-up

To study breast carcinogenesis, we used the dimethylbenz[*a*]anthracene (DMBA)-induced mammary carcinogenesis model. To increase the yield of mice with DMBA-induced mammary tumors and to decrease the latency for tumor development, the protocol as described by Aldaz et al. [30] was used. Briefly, 14 *IGFBP-3* wild-type ($BP3^{+/+}$) and 15 knockout ($BP3^{-/-}$) female mice at 6 weeks old received a subcutaneous implant in the interscapular area of two compressed pellets of medroxyprogesterone acetate (MPA), 20 mg each (Hormone Pellet press, Kansas City, KS). Then they were given DMBA by gavage (a total of 4 doses of 1 mg of DMBA in 0.1 ml of sesame oil when they were 9, 10, 12, and 13 weeks of age). Three animals of each genotype were in the control group receiving only MPA and the vehicle (sesame oil). Mice were kept for up to 13 months after the last DMBA treatment. Palpable tumors were monitored weekly and measured with a caliper. Mice were also monitored for behavioral changes, weight loss (>20 %), and dehydration. At the end of the experiment or when tumors reach 1 cm^3, the animals were anesthetized, blood was collected by cardiac puncture, the animals were euthanized by cervical dislocation, and then tumors and tissue were collected and frozen until use.

Table 1 Primers for the genotyping of IGFBP-3 mice

Primer sequences	
UTT022-7	5′-TGCAGGCAGCCTAAGCACCTACCTC
UTT022-8	5′-CCCAGGGTCCATTTTCCAACCTT
UTT022-15	5′-TAAGGTTCTCCAGACCTCAAAGTG
GTI	5′-CCCTAGGAATGCTCGTCAAGA

Mouse DNA was obtained from tail snip and genotyping was performed by PCR using the above primers

Metastasis assay

Five $BP3^{+/+}$ and 5 $BP3^{-/-}$ female mice (on a Balb/c background) between 8 and 10 weeks of age, were injected in the tail vein with 10^5 4T1 mouse breast cancer cells, purchased from American Type Culture Collection, Manassas, VA). 16 days post-injection, mice were anesthetized, blood was collected by cardiac puncture, and then the lungs were perfused with PBS and fixed in Bouin's solution. The number of lung nodules, as well as their histopathology, was established by two independent and blinded pathologists. This experiment was repeated twice, with similar results.

Western blotting

Tissue lysates were prepared in lysis buffer (50 mM Hepes, 150 mM NaCl, 1 % Triton-X 100, 0.02 % sodium azide, 60 mM β-glycerophosphate, 1 mM DTT, protease inhibitor cocktail (Complete tablets, Roche, Laval, QC, Canada) at pH 7.2, and 1.46 μM pepstatin A (BioShop Canada Inc., Burlington, ON, Canada) added just before use). The protein concentration in the supernatant fraction was determined and the extracts were stored at −80 °C. Proteins (20 μg for tumors and 50 μg for serum samples) were resolved electrophoretically on denaturing SDS–polyacrylamide gels (10 or 12 %), transferred to nitrocellulose membranes, and probed with the following antibodies overnight at 4 °C: anti-IGFBP-3 (R&D Systems Inc., Minneapolis, MN), anti-IGFBP-2, and anti-transferrin (Santa Cruz Biotechnology, Inc., Santa Cruz, CA), anti-IGFBP-5 (Novus Biologicals, Littleton, CO), anti-phospho-AKT^{Ser473}, anti-AKT, anti-IGF-1

receptor, anti-poly(ADP ribose) polymerase (PARP), anti-phsopho-MAPK$^{T202/Y204}$, anti-MAPK, anti-ribosomal protein S6 (S6), anti-phospho-S6$^{S235/236}$, and anti-β-actin (Cell Signaling Technology, Beverly, MA) antibodies. The position of the proteins was visualized with the appropriate horseradish peroxidase-conjugated anti-rabbit, anti-goat, or anti-rat immunoglobulin antibodies (ECL, GE Healthcare LifeScience, Baie d'Urfé, QC, Canada). Four different westerns were done for each protein with tumor samples from 2 different protein lysates for all ($n = 12$ for BP3$^{+/+}$ and $n = 9$ for BP3$^{-/-}$). Densitometry was calculated using both a scanner and computer program according to

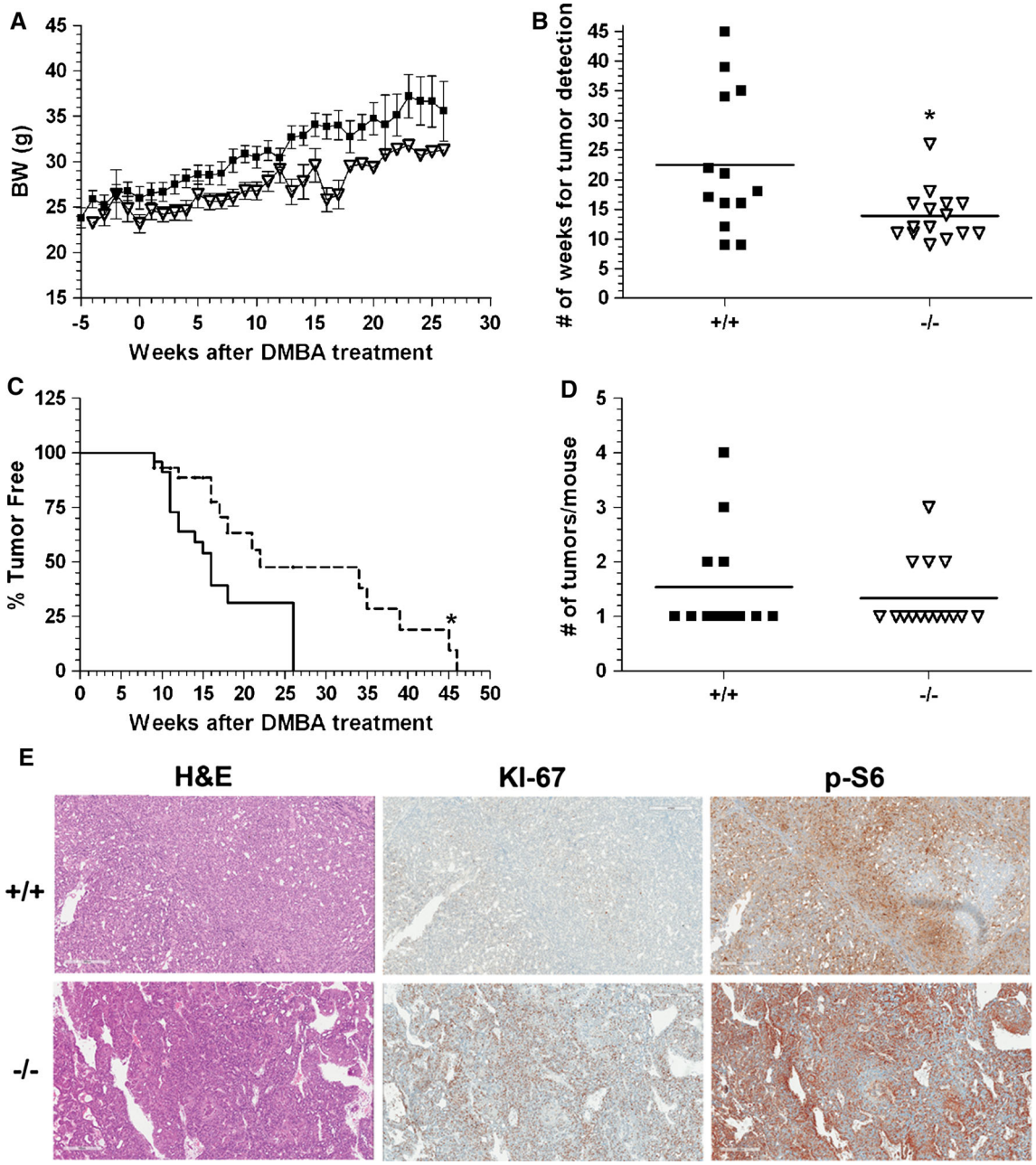

Fig. 1 IGFBP-3 knockout mice develop tumors earlier than wild-type IGFBP-3 mice. **a** Body weight curve of both groups, determined weekly (overall significance of difference between groups: $P < 0.0001$); **b** after DMBA treatment, time of first appearance of palpable tumors was monitored twice weekly (*asterisk* $P = 0.0144$ for difference between groups); **c** percentage of mice without tumors as a function of time post carcinogen exposure, according to genotype. *Dotted line* BP3$^{+/+}$, *solid line* BP3$^{-/-}$ mice (*asterisk* $P = 0.0144$ for difference between groups; **d** at the time of euthanasia, the number of mammary tumors was counted for each mouse. The number of tumors per mouse was not different ($P = 0.5555$). *Square* BP3$^{+/+}$; *open inverted triangle* BP3$^{-/-}$ mice. **e** Representative H & E and immunohistochemistry of Ki-67 and phospho-S6$^{S240/244}$ antibodies of breast tumors for both groups ($n = 5$). +/+ BP3$^{+/+}$; −/− BP3$^{-/-}$. Magnitude X200

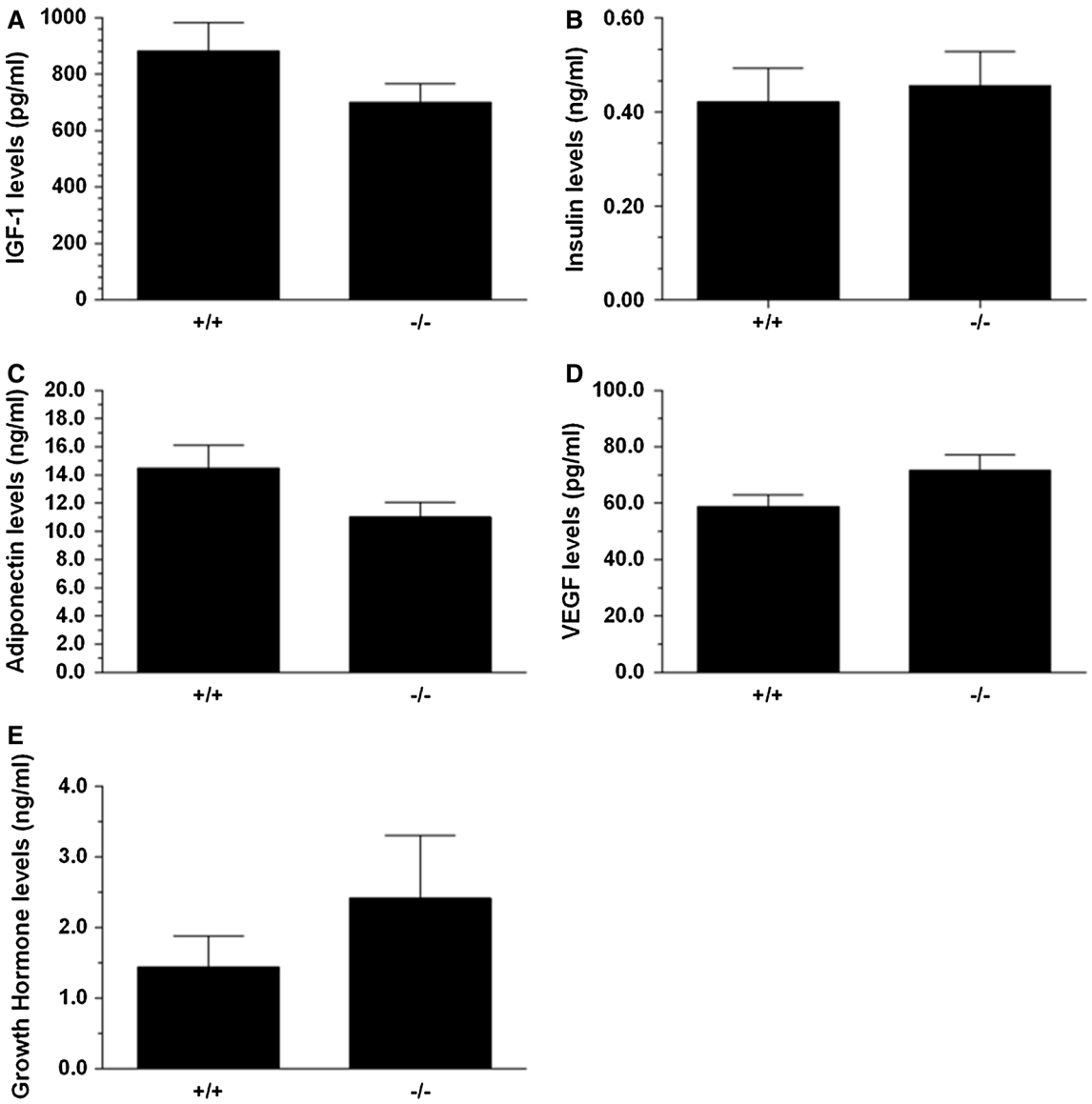

Fig. 2 Circulating hormone levels are similar between the two groups. **a** IGF-1 levels; **b** insulin levels; **c** adiponectin levels; **d** VEGF levels; **e** growth hormone levels. Blood was collected at the time of euthanasia from non-fasting $BP3^{-/-}$ and $BP3^{+/+}$ mice. Differences between the two groups were non-statistically significant. *Data* presented are the mean ± SEM

manufacturers' instructions. The density of the bands was normalized to the percent density of β-actin for IGFBP-5 or to total AKT protein for phospho-AKT^{S473} in the tumors and to the percent density of transferrin for IGFBP-2, IGFBP-3, and IGFBP-5 in the serum.

Ligand blotting

Serum samples (50 μg—equivalent of ~2 μl) were diluted in non-reducing loading buffer, heated for 5 min at 50 °C, run on 12 % polyacrylamide gel, and transferred on nitrocellulose membrane as for Western blotting. The non-radioactive ligand blotting was carried out according to the manufacturer's protocols (#IGF005, IBT Systems, Reutlingen, Germany) and the detection of the IGFBPs was done with ECL reagents as for the Western blotting in two independent experiments ($n = 4$). Densitometry was calculated using both a scanner and computer program according to manufacturers' instructions. The density of the bands for each sample was added to get the density of the total amount of IGFBPs.

Insulin, adiponectin, IGF-1, VEGF, and growth hormone (GH) ELISA

Hormone serum levels were measured in duplicate using rodent insulin ($n = 13$ for both $BP3^{+/+}$ and for $BP3^{-/-}$), VEGF ($n = 7$ for $BP3^{+/+}$ and $n = 12$ for $BP3^{-/-}$), and

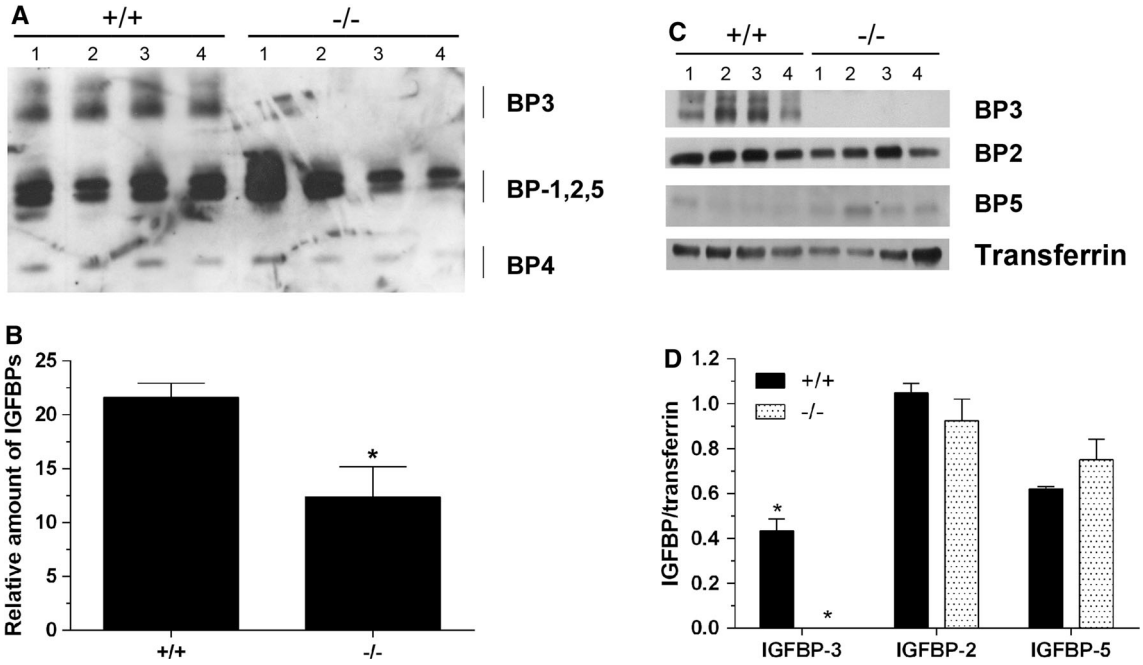

Fig. 3 IGFBP-3 knockout: IGFBPs do not compensate for the absence of IGFBP-3. **a** The distribution of the IGFBPs in both genotypes was determined by western ligand blots of serum. **b** Densitometry of ligand blot to determine the total IGFBPs levels for both $BP3^{+/+}$ and $BP3^{-/-}$. *asterisk* $P = 0.0368$. Data presented are the mean ± SEM. **c** Western analysis was performed to evaluate individually the levels of IGFBPs (anti-IGFBP-2, anti-IGFBP-3, anti-IGFBP-5, and anti-transferrin (loading control) antibodies) in serum. **d** Densitometry of (C) *asterisk* $P = 0.0036$. Data presented are the mean ± SEM. Representative western and western ligand blots are presented. Numbers 1–4 correspond each to an individual animal sample

GH ($n = 7$ for $BP3^{+/+}$ and $n = 9$ for $BP3^{-/-}$) and mouse adiponectin ($n = 12$ for $BP3^{+/+}$ and $n = 13$ for $BP3^{-/-}$) immunoassays (Millipore Corp., Etobicoke, ON, Canada) and rodent IGF-1 ELISA ($n = 13$ for both $BP3^{+/+}$ and for $BP3^{-/-}$) (Diagnostic Systems Laboratories, Webster, TX), according to the manufacturer's protocols.

Immunohistochemistry staining and histopathology

Immunohistochemistry (IHC) was performed at the Segal Cancer Centre Research Pathology Facility (Jewish General Hospital, Montreal, QC, Canada). Tissue samples were cut at 4-μm, placed on SuperFrost/Plus slides (Fisher Scientific, Ottawa, ON, Canada) and dried overnight at 37 °C, before IHC processing. The slides were then loaded onto the Discovery XT Autostainer (Ventana Medical System, Inc., Tucson, AZ). All solutions used for automated immunohistochemistry were from Ventana Medical System unless otherwise specified. Slides underwent de-paraffinization, heat-induced epitope retrieval (CC1 prediluted solution Ref: 950-124, standard protocol). Immunostaining was performed online using a heat protocol. Briefly, rabbit polyclonal anti-Ki-67 (Novus, Oakville, ON, Canada) diluted at (1:100) and rabbit monoclonal anti-ribosomal protein $S6^{S240/244}$ (Cell Signaling Technology) (1:1000) in the antibody diluent (Ref: 251-018) were manually applied for 32 min at 37 °C then followed by the appropriate detection kit (OmniMap anti-Rabbit-HRP, Ref: 760-4311) for 8 min, followed by ChromoMap-DAB Ref: 760-159). A negative control was performed by omission of the primary antibody. Slides were counterstained with Hematoxylin for 4 min, blued with Bluing Reagent for 4 min, removed from the autostainer, washed in warm soapy water, dehydrated through graded alcohols, cleared in xylene, and mounted with Permount. Slides were scanned at ×20 using a ScanScope AT Turbo (Leica Biosystems, Concord, ON, Canada) with default settings. They were analyzed for phospho-$S6^{S240/244}$ and Ki-67 using the Aperio ePathology Cytoplasmic v2 algorithm (Leica Biosystems) with default input parameters. Tumors ($n = 11$ for $BP3^{+/+}$ and $n = 9$ for $BP3^{-/-}$) and lungs ($n = 5$ for both $BP3^{+/+}$ and for $BP3^{-/-}$) were sectioned and stained with hematoxylin and eosin. Two blinded evaluators from the pathology department determined the tumor type for each sample.

Statistical analyses

The data presented are mean ± SEM. For insulin, adiponectin, VEGF, GH, and IGF-1 levels, a nonparametric

procedure (Mann–Whitney–Wilcoxon (MWW)) was used to perform an analysis of variance on ranks where data were not normally distributed. For tumor detection and number of tumor graphs, a one-way analysis of variance was used to determine if a significant difference was among all treatment groups. For survival graph, Log-rank test using the LifeTest procedure was used to analyze Kaplan–Meier curve and statistical significance for body weight graph was evaluated using Proc Mixed Procedure. All statistical analyses were performed using Statistical Analysis System software, version 9.2 (SAS Institute, Cary, NC), with P values < 0.05 considered significant.

Results and discussion

Female mice of each genotype (*IGFBP-3*$^{-/-}$ and *IGFBP-3*$^{+/+}$) were followed for up to 13 months after the last DMBA gavage. *IGFBP-3* knockout mice showed no obvious phenotype compared to wild-type mice, except that with time, the *IGFBP-3*$^{-/-}$ mice weighed less than *IGFBP-3*$^{+/+}$ mice (Fig. 1a: 30.06 ± 4.19 g versus 32.79 ± 5.23 g at sacrifice time, $P < 0.0001$).

There was a major difference in the time of first appearance of mammary tumors, which was earlier in BP3$^{-/-}$ mice (13.9 ± 1.1 weeks versus 22.5 ± 3.3 weeks, $P = 0.0144$) (Fig. 1b–c). However, there was no difference in the number of tumors per mouse between the two groups (BP3$^{-/-}$: 1.33 ± 0.16 versus BP3$^{+/+}$: 1.54 ± 0.27 tumors, $P = 0.5555$) (Fig. 1d). Histopathologic analyses of the primary tumors showed that in the BP3$^{-/-}$ mice, 80.0 % were invasive ductal carcinomas and 20.0 % were adenosquamous carcinomas. As for tumors in BP3$^{+/+}$ mice, 77.8 % were invasive ductal carcinomas, 22.2 % were poorly differentiated adenocarcinomas, and 11.1 % were defined as adenosquamous carcinomas. Representative histology photographs for both genotypes are shown in Fig. 1e. This is consistent with previous publications [30, 31].

The mitotic index was determined using Ki-67. Cell proliferation was higher in tumors from BP3$^{-/-}$ mice compared with BP3$^{+/+}$ mice (26.92 % ± 5.23 versus 13.26 % ± 3.72, respectively; $P = 0.05$). However, the percentage of positive cells for phospho-S6$^{Ser240/244}$ was not statistically different between both groups: 57.11 % ± 7.49 versus 75.80 % ± 5.67 ($P = 0.06$) (Fig. 1e).

An important function of IGFBP-3 is to act as a carrier protein for IGFs in the circulation by the formation of a stable complex with IGF-1 and the acid labile subunit (ALS) protein, an interaction which prolongs the half-life of the growth factors in the circulation. We measured by ELISA circulating total IGF-1 levels and found that they were not significantly different between the two groups: 700.2 ± 65.9 pg/ml versus 881.8 ± 101.7 pg/ml, respectively, for BP3$^{-/-}$ and BP3$^{+/+}$ mice (Fig. 2a). The trend toward higher IGF-1 levels in the control mice is likely due to reduced serum half-life of IGF-1 in the absence of IGFBP-3. We cannot exclude the possibility that the proportion of free-IGF-1 uncomplexed with binding proteins in the tissue microenvironment of primary tumor sites could be higher in the knockout animals compared with wild-type. Levels of insulin (0.456 ± 0.073 versus 0.421 ± 0.071 ng/ml), adiponectin (11.02 ± 1.05 versus 14.52 ± 1.59 ng/ml), and VEGF (71.60 ± 5.64 versus 58.76 ± 4.24 pg/ml) were also similar in BP3$^{-/-}$ as in BP3$^{+/+}$ mice, respectively (Fig. 2b–d). The levels of circulating GH were also measured (Fig. 2e). No statistical significant difference was observed, although a trend toward higher GH levels was observed in BP3$^{-/-}$ compared with BP3$^{+/+}$ mice (2.41 ± 0.89 versus 1.44 ± 0.44 ng/ml). However, since it is well-known that GH levels vary in a pulsatile manner, measurements at a single time point

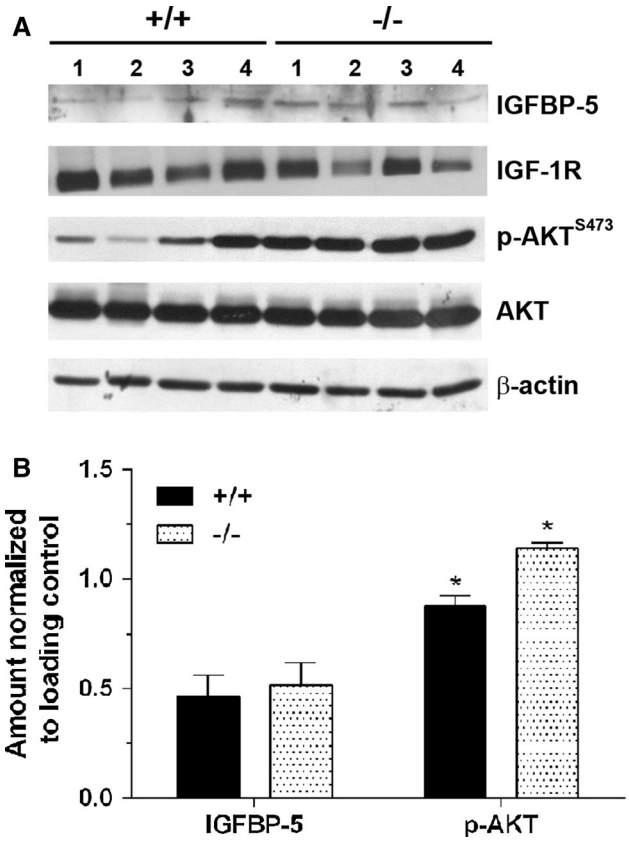

Fig. 4 Effects on signaling downstream of the IGF-1 receptor in breast tumors. **a** At the end of the experiment, tumors were collected and snap frozen. Cell lysates were prepared and proteins were processed by Western blot analysis with anti-IGFBP-5, anti-phospho-Akt^{Ser473}, anti-total Akt, anti-total IGF-1R, and anti-β-actin (as loading control) antibodies. **b** Densitometry graphs of (**a**). *asterisk* $P = 0.0038$. Representative western blots are presented. Data presented are the mean ± SEM. Numbers 1–4 correspond each to an individual animal sample

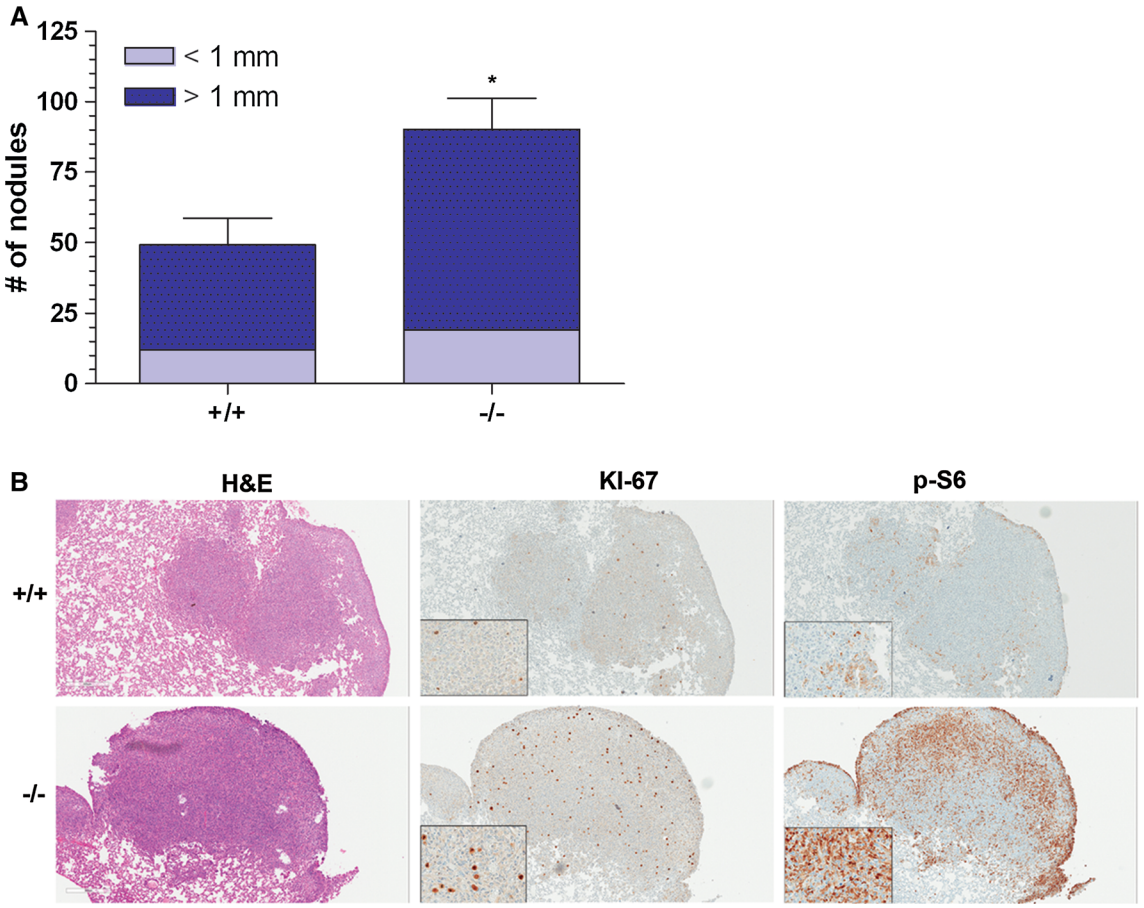

Fig. 5 Effects of IGFBP-3 on lung metastasis of 4T1 cells. 4T1 cells were injected in the tail vein to both $BP3^{-/-}$ and $BP3^{+/+}$ mice. **a** Nodules on lungs were counted 16 days post-injection, distinguishing between nodules smaller or larger than 1 mm, *asterisk* $P = 0.0159$. *Data* presented are the mean ± SEM. **b** Representative H & E and immunohistochemistry of Ki-67 and phospho-$S6^{S240/244}$ antibodies of lung metastasis for both groups ($n = 5$). +/+ $BP3^{+/+}$; −/− $BP3^{-/-}$. Magnitude ×200; *insert* ×400

provide limited information concerning growth hormone profiles over time.

To better understand the mechanisms responsible for the difference in time for tumor appearance, western ligand blots were performed to determine if circulating levels of other IGFBPs increased to compensate for the absence of IGFBP-3. Figure 3a shows that in some *IGFBP-3* knockout mice the amount of IGFBP-1, 2, or 5 was increased, but that there was considerable variability. As for IGFBP-4, no increase was observed in the knockout mice. Densitometry was done to determine whether total IGFBPs levels were similar between both groups. Total IGFBPs levels were lower in $BP3^{-/-}$ than in $BP3^{+/+}$ mice (Fig. 3b). There is evidence for some compensatory increase in other IGFBPs. Since by western ligand analysis, one cannot differentiate between IGFBP-1, 2, and 5, conventional western blots were used to assess the intensity of individual binding proteins in the serum of each genotype (Fig. 3c). No difference was observed between $BP3^{+/+}$ and $BP3^{-/-}$ mice for IGFBP-2; however, there was a trend for IGFBP-5 band intensity to be higher in $BP3^{-/-}$ than in $BP3^{+/+}$ mice, suggesting that IGFBP-5 level may increase to compensate to some extent for the loss of IGFBP-3 (Fig. 3d).

In the tumor samples, IGF-1R downstream signaling was analyzed and there was a significant increase in phosphorylation of AKT^{Ser473} in $BP3^{-/-}$ mice, but no obvious difference in levels of total AKT or total IGF-1R proteins (Fig. 4). Interestingly, in the tumors, there seems be an increase in IGFBP-5 in the IGFBP-3 knockout compared with the wild-type mice. No difference was observed in the phosphorylation levels of $MAPK^{T202/Y204}$ and $S6^{S235/236}$ proteins, nor in the levels of the cleaved PARP protein, marker of apoptosis, between the 2 groups (data not shown).

To determine whether *IGFBP-3* has a role in breast cancer cell metastasis to the lungs, we used the murine 4T1 mammary cell line model, as described in the "Materials and methods" section. Figure 5a shows that the number of metastatic nodules on lungs of *IGFBP-3*$^{-/-}$ mice was significantly higher as compared to the number of nodules on *IGFBP-3*$^{+/+}$ lungs (88.3 ± 14.0 versus 49.2 ± 12.9

nodules, respectively, $P = 0.0159$). With respect to nodule size, $BP3^{-/-}$ mice had a higher percentage of nodules larger than 1 mm compared to $BP3^{+/+}$ mice (80.6 % versus 75.6 %, respectively). Histopathology showed ductal carcinoma for both $BP3^{-/-}$ and $BP3^{+/+}$ hosts (Fig. 5b). Proliferation was assayed using Ki-67 marker: a non-significant trend toward higher Ki-67 in $BP3^{-/-}$ mice was observed (2.86 % ± 0.31, versus 2.62 % ± 0.40, $P = 0.659$). However, results obtained for phospho-$S6^{S240/244}$ labeling showed higher activation for the $BP3^{-/-}$ mice (29.39 % ± 6.89 versus 8.09 % ± 4.25, respectively; $P = 0.0281$ (Fig. 5b).

The difference in signaling downstream of the IGF-1 receptor in tumors of $BP3^{-/-}$ and $BP3^{+/+}$ mice at the time of sacrifice was modest in magnitude relative to the difference in number of metastasis. This raises the possibility that I*GFBP-3* knockout may influence early steps in the metastatic process. The results from the metastasis assay suggest that *IGFBP-3* has a role as metastasis suppressor gene, and that any increase in IGFBP-5 was not sufficient to abrogate the effect of the absence of IGFBP-3 on the metastasis endpoint. Our results are consistent with previous published data for metastasis models of other tissues: in a prostate cancer model, using the transgenic PB-Hi-Myc mice crossed with an *IGFBP-3* knockout mouse model [28] showed that the absence of IGFBP-3 increased metastasis to distant organs. In other in vitro models, IGFBP-3 inhibited migration of endometrial cancer cells [32] and was involved in inhibiting anchorage-independent growth [33], which could favor a metastatic process.

Although *IGFBP-3* knockout does not lead to major phenotypic differences compared to wild-type mice under control conditions, our results, for the first time, reveal that the *IGFBP-3* knockout mice differ from controls in terms of mammary tumor growth following exposure to DMBA and in a model of breast tumor cell metastasis. The small decrease in body weight we observed in the absence of IGFBP-3 implies that at the whole-organism level, IGFBP-3 serves to increase IGF activity, perhaps by prolonging serum half-life. This result is consistent with prior reports [27, 34]. Previous studies have shown that a decrease in GH/IGF-1 levels reduced tumor development in several models [34–37]. On the other hand, in the context of DMBA-induced carcinogenesis and of metastasis, our data demonstrate that knockout of *IGFBP-3* increases tumor aggressiveness, without a major change in GH or IGF-1 serum levels. Our observations thus support the hypothesis that IGFBP-3 influences neoplasia by reducing IGF-1 bioactivity and/or by direct IGF-independent actions [1–11].

Clinically, it is well-known that there is considerable person-to person heterogeneity in IGFBP-3 serum levels, and some of this variability is attributable to polymorphisms in the *IGFBP-3* promoter [38, 39]. This variation has not been consistently associated with breast cancer risk or outcome. A likely explanation for this is that the variation within the normal range would be expected to have more subtle effects on neoplasia than the extreme variation used in the *IGFBP-3* knockout model.

Acknowledgments We would like to thank Ms. Véronique Michaud and Mr. Yvhans Chery for their technical assistance with the animal care, Dr. Naciba Benlimame and Ms. Lilian Canetti for their collaboration for the immunohistochemistry procedures and Ms Jasmin Sander for the scanning of the slides. We are also grateful to Ms. Rhoda Lim for her help in the submission of this manuscript.

Conflict of interest Dr. David R. Powell is the Vice-President of Metabolism Research at Lexicon Pharmaceuticals, Inc., of which the knockout mice were generated. The other authors have no conflict of interest to disclose.

Funding Miguel Bazile was supported through the McGill Integrated Cancer Research Training Program Studentship.

References

1. Firth SM, Baxter RC (2002) Cellular actions of the insulin-like growth factor binding proteins. Endocr Rev 23:824–854
2. Hwa V, Oh Y, Rosenfeld RG (1999) The insulin-like growth factor-binding protein (IGFBP) superfamily. Endocr Rev 20:761–787
3. Jogie-Brahim S, Feldman D, Oh Y (2009) Unraveling insulin-like growth factor binding protein-3 actions in human disease. Endocr Rev 30(5):417–437
4. Pollak MN, Schernhammer ES, Hankinson SE (2004) Insulin-like growth factors and neoplasia. Nat Rev Cancer 4(7):505–518
5. Lu Y, Zi X, Zhao Y, Mascarenhas D, Pollak M (2001) Insulin-like growth factor-I receptor signaling and resistance to trastuzumab (Herceptin). J Natl Cancer Inst 93:1852–1857
6. Nickerson T, Huynh H, Pollak M (1997) Insulin-like growth factor binding protein-3 induces apoptosis in MCF7 breast cancer cells. Biochem Biophys Res Commun 237:690–693
7. Pratt S, Pollak M (1994) Insulin-like growth factor binding protein 3 inhibits estrogen-stimulated breast cancer cell proliferation. Biochem Biophys Res Commun 198:292–297
8. Shen L, Dean NM, Glazer RI (1999) Induction of p53-dependent, insulin-like growth factor-binding protein-3-mediated apoptosis in glioblastoma multiforme cells by a protein kinase Calpha antisense oligonucleotide. Mol Pharmacol 55:396–402
9. Butt AJ, Williams DC (2001) IGFBP-3 and apoptosis—a licence to kill? Apoptosis 6:199–205
10. Gill ZP, Perks CM, Newcomb PV, Holly JM (1997) Insulin-like growth factor-binding protein (IGFBP-3) predisposes breast cancer cells to programmed cell death in a non-IGF-dependent manner. J Biol Chem 272:25602–25607
11. Hong J, Zhang G, Dong F, Rechler MM (2002) Insulin-like growth factor (IGF)-binding protein-3 mutants that do not bind IGF-I or IGF-II stimulate apoptosis in human prostate cancer cells. J Biol Chem 277:10489–10497
12. McCaig C, Fowler CA, Laurence NJ, Lai T, Savage PB, Holly JMP, Perks CM (2002) Differential interactions between IGFBP-3 and transforming growth factor-beta (TGF-beta) in normal vs cancerous breast epithelial cells. Br J Cancer 86:1963–1969
13. Williams AC, Collard TJ, Perks CM, Newcomb P, Moorghen M, Holly JMP, Paraskeva C (2000) Increased p53-dependent

apoptosis by the insulin-like growth factor binding protein IGFBP-3 in human colonic adenoma-derived cells. Cancer Res 60:22–27
14. Liu B, Lee KW, Anzo M, Zhang B, Zi X, Tao Y, Shiry L, Pollak M, Lin S, Cohen P (2007) Insulin-like growth factor-binding protein-3 inhibition of prostate cancer growth involves suppression of angiogenesis. Oncogene 26:1811–1819
15. Gucev ZS, Oh Y, Kelley KM, Rosenfeld RG (1996) Insulin-like growth factor binding protein 3 mediates retinoic acid and transforming growth factor beta 2-induced growth inhibition in human breast cancer cells. Cancer Res 56:1545–1550
16. Huynh HT, Robitaille G, Turner JD (1991) Establishment of bovine mammary epithelial cells (MAC-T): an in vitro model for bovine lactation. Exp Cell Res 197:191–199
17. Huynh HT, Yang XF, Pollak M (1996) Estradiol and antiestrogens regulate a growth inhibitory insulin-like growth factor binding protein 3 autocrine loop in human breast cancer cells. J Biol Chem 271:1016–1021
18. Khandwala HM, McCutcheon IE, Flyvbjerg A, Friend KE (2000) The effects of insulin-like growth factors on tumorigenesis and neoplastic growth. Endocr Rev 21:215–244
19. Martin JL, Coverley JA, Pattison ST, Baxter RC (1995) Insulin-like growth factor-binding protein-3 production by MCF-7 breast cancer cells: stimulation by retinoic acid and cyclic adenosine monophosphate and differential effects of estradiol. Endocrinology 136:1219–1226
20. Torrisi R, Parodi S, Fontana V, Pensa F, Casella C, Barreca A, De P, Costa A, Decensi A (1998) Effect of fenretinide on plasma IGF-I and IGFBP-3 in early breast cancer patients. Int J Cancer 76:787–790
21. Burrows C, Shiry LJ, Holly JMP, Perks CM (2003) Differential effects of IGFBP-3 on apoptosis of breast epithelial cells according to apoptotic trigger. Growth Hormone and IGF Research 13 (Abstract P28):203–222
22. Fowler CA, Perks CM, Newcomb PV, Savage PB, Farndon JR, Holly JM (2000) Insulin-like growth factor binding protein-3 (IGFBP-3) potentiates paclitaxel-induced apoptosis in human breast cancer cells. Int J Cancer 88:448–453
23. Neuenschwander S, Schwartz A, Wood TL, Roberts CT Jr, Hennighausen L, LeRoith D (1996) Involution of the lactating mammary gland is inhibited by the IGF system in a transgenic mouse model. J Clin Investig 97(10):2225–2232
24. Schneider MR, Lahm H, Wu M, Hoeflich A, Wolf E (2000) Transgenic mouse models for studying the functions of insulin-like growth factor-binding proteins. FASEB J 14(5):629–640
25. Silha JV, Murphy LJ (2002) Insights from insulin-like growth factor binding protein transgenic mice. Endocrinology 143(10): 3711–3714
26. Silha JV, Sheppard PC, Mishra S, Gui Y, Schwartz J, Dodd JG, Murphy LJ (2006) Insulin-like growth factor (IGF) binding protein-3 attenuates prostate tumor growth by IGF-dependent and IGF-independent mechanisms. Endocrinology 147(5):2112–2121
27. Ning Y, Schuller AG, Bradshaw S, Rotwein P, Ludwig T, Frystyk J, Pintar JE (2006) Diminished growth and enhanced glucose metabolism in triple knockout mice containing mutations of insulin-like growth factor binding protein-3, -4, and -5. Mol Endocrinol 20(9):2173–2186
28. Mehta HH, Gao Q, Galet C, Paharkova V, Wan J, Said J, Sohn JJ, Lawson G, Cohen P, Cobb LJ, Lee KW (2011) IGFBP-3 is a metastasis suppression gene in prostate cancer. Cancer Res 71(15):5154–5163
29. Lue Y, Swerdloff R, Liu Q, Mehta H, Hikim AS, Lee KW, Jia Y, Hwang D, Cobb LJ, Cohen P, Wang C (2010) Opposing roles of insulin-like growth factor binding protein 3 and humanin in the regulation of testicular germ cell apoptosis. Endocrinology 151(1): 350–357
30. Aldaz CM, Liao QY, LaBate M, Johnston DA (1996) Medroxyprogesterone acetate accelerates the development and increases the incidence of mouse mammary tumors induced by dimethylbenzanthracene. Carcinogenesis 17(9):2069–2072
31. Siddiqui RA, Harvey KA, Walker C, Altenburg J, Xu Z, Terry C, Camarillo I, Jones-Hall Y, Mariash C (2013) Characterization of synergistic anti-cancer effects of docosahexaenoic acid and curcumin on DMBA-induced mammary tumorigenesis in mice. BMC Cancer 13:418. doi:10.1186/1471-2407-13-418
32. Gribben L, Baxter RC, Marsh DJ (2012) Insulin-like growth factor binding protein-3 inhibits migration of endometrial cancer cells. Cancer Lett 317(1):41–48. doi:10.1016/j.canlet.2011.11.011
33. Chun SY, Chen F, Washburn JG, MacDonald JW, Innes KL, Zhao R, Cruz-Correa MR, Dang LH, Dang DT (2007) CDX2 promotes anchorage-independent growth by transcriptional repression of IGFBP-3. Oncogene 26(32):4725–4729. doi:10.1038/sj.onc.1210258
34. Saldana SM, Lee HH, Lowery FJ, Khotskaya YB, Xia W, Zhang C, Chang SS, Chou CK, Steeg PS, Yu D, Hung MC (2013) Inhibition of type I insulin-like growth factor receptor signaling attenuates the development of breast cancer brain metastasis. PLoS One 8(9):e73406. doi:10.1371/journal.pone.0073406
35. Gahete MD, Cordoba-Chacon J, Lantvit DD, Ortega-Salas R, Sanchez-Sanchez R, Perez-Jimenez F, Lopez-Miranda J, Swanson SM, Castano JP, Luque RM, Kineman RD (2014) Elevated GH/IGF-I promotes mammary tumors in high-fat, but not low-fat, fed mice. Carcinogenesis. doi:10.1093/carcin/bgu161
36. Pollak M, Blouin MJ, Zhang JC, Kopchick JJ (2001) Reduced mammary gland carcinogenesis in transgenic mice expressing a growth hormone antagonist. Br J Cancer 85(3):428–430. doi:10.1054/bjoc.2001.1895
37. Ramsey MM, Ingram RL, Cashion AB, Ng AH, Cline JM, Parlow AF, Sonntag WE (2002) Growth hormone-deficient dwarf animals are resistant to dimethylbenzanthracine (DMBA)-induced mammary carcinogenesis. Endocrinology 143(10):4139–4142. doi:10.1210/en.2002-220717
38. Deal C, Ma J, Wilkin F, Paquette J, Rozen F, Ge B, Hudson T, Stampfer M, Pollak M (2001) Novel promoter polymorphism in insulin-like growth factor-binding protein-3: correlation with serum levels and interaction with known regulators. J Clin Endocrinol Metab 86(3):1274–1280
39. Jernstrom H, Wilkin F, Deal C, Chu W, Tao Y, Majeed N, Narod S, Hudson T, Pollak M (2001) Genetic and non-genetic factors associated with variation of plasma levels of insulin-like growth factor-I and insulin-like growth factor binding protein-3 in healthy premenopausal women. Cancer Epidemiol Biomark Prev 10:377–384